PNAS RESEARCH ARTICLE | APPLIED BIOLOGICAL SCIENCES OPEN ACCESS

Intratumoral injection of schwannoma with attenuated *Salmonella typhimurium* induces antitumor immunity and controls tumor growth

Sherif G. Ahmed[a], Giulia Oliva[a,b], Manlin Shao[a], Xinhui Wang[c], John J. Mekalanos[b,1], and Gary J. Brenner[a,1]

Contributed by John J. Mekalanos; received February 22, 2022; accepted April 13, 2022; reviewed by Samuel Miller and Daniel Portnoy

Schwannomas are slow-growing benign neoplasms that develop throughout the body causing pain, sensory/motor dysfunction, and death. Because bacterial immunotherapy has been used in the treatment of some malignant neoplasms, we evaluated attenuated *Salmonella typhimurium* strains as immunotherapies for benign murine schwannomas. Several bacterial strains were tested, including VNP20009, a highly attenuated strain that was previously shown to be safe in human subjects with advanced malignant neoplasms, and a VNP20009 mutant that was altered in motility and other properties that included adherence and invasion of cultured mammalian cells. VNP20009 controlled tumor growth in two murine schwannoma models and induced changes in cytokine and immune effector cell profiles that were consistent with induction of enhanced innate and adaptive host immune responses compared with controls. Intratumoral (i.t.) injection of *S. typhimurium* led to tumor cell apoptosis, decreased tumor angiogenesis, and lower growth of the injected schwannoma tumors. Invasive VNP20009 was significantly more efficacious than was a noninvasive derivative in controlling the growth of injected tumors. Bacterial treatment apparently induced systemic antitumor immunity in that the growth of rechallenge schwannomas implanted following primary bacterial treatment was also reduced. Checkpoint programmed death-1 (PD-1) blockade induced by systemic administration of anti–PD-1 antibodies controlled tumor growth to the same degree as i.t. injection of *S. typhimurium*, and together, these two therapies had an additive effect on suppressing schwannoma growth. These experiments represent validation of a bacterial therapy for a benign neoplasm and support development of *S. typhimurium* VNP20009, potentially in combination with PD-1 inhibition, as a schwannoma immunotherapy.

schwannoma | attenuated bacterial vaccines | *Salmonella typhimurium* | checkpoint blockade

Significance

Neurofibromatosis type 2 (NF2) is caused by slow-growing benign schwannomas that develop throughout the body and cause severe pain, morbidity, and mortality. Surgical resection and radiotherapy are the standards of care for NF2 but have major limitations. The paucity of NF2 therapeutic options is a major unmet medical need. Here, we show that bacteriotherapy immunotherapy using an attenuated strain of *Salmonella typhimurium* can control this neoplasm in a preclinical mouse model. This strategy decreased angiogenesis and the volume of the injected tumor and induced a systemic immune response as well as an immunological memory response that targeted distal tumors and prevented development of new lesions. These results support the evaluation of attenuated *S. typhimurium* as a treatment for NF2 disease.

Schwannomas are slow-growing benign neoplasms derived from Schwann-lineage cells that typically first appear in childhood and adolescence (1). Depending on location and size, these tumors can cause a variety of gain- and loss-of-function neurological deficits including hearing loss, imbalance, tinnitus, motor loss, severe pain (2), and in some cases, fatal brainstem compression (3). Schwannomas may arise sporadically ("sporadic schwannoma") or from the debilitating genetic syndromes neurofibromatosis type 2 (NF2) and schwannomatosis (4). Surgical resection and symptomatic management of pain are the main treatments for schwannoma. Resection often causes additional neurologic damage, is typically noncurative, and may be impractical due to location or large numbers of tumors (5). Conventional anticancer therapeutics are not effective against these benign lesions because schwannoma cells replicate slowly (6). Bevacizumab is the only generally accepted pharmacotherapy for schwannoma; it stabilizes tumor growth temporarily in a subset of tumors by targeting the highly vascularized nature of these neoplasms (7). Current strategies for pain control are inadequate for many patients, and treatment is further complicated as schwannomas appear in multiple locations in a given individual, with new lesions developing throughout life. Thus, current treatments cannot relieve the lifelong suffering caused by schwannomas in affected patients.

In the mid-1800s, William Coley introduced bacterial cancer therapy (BCT) using live *Streptococcus pyogenes* to treat solid tumors (8). Some bacterial strains, including *Salmonella typhimurium* (9–12), specifically home to and proliferate within hypoxic areas of angiogenic tumors, inducing direct lysis of tumor cells and antitumor immune responses (13). Furthermore, bacterial injection of tumors inhibits angiogenesis (14), shifts tumoral macrophages from M2 (tumor promoting) to M1 (tumoricidal) types (11, 15), and induces antitumor adaptive immunity (16).

Despite this promising preclinical evidence, results from clinical trials of BCT have been disappointing (17, 18). This lack of efficacy may be due to the rapid division rates

Competing interest statement: S.G.A. and G.J.B. have filed a patent application with the US Patent and Trademark Organization related to this work. G.J.B. and J.J.M. have a financial interest in Mulberry Biotherapeutics, Inc., a company developing novel biologic therapies for schwannoma and related neoplasms. The research presented here was partially supported by a grant from the NIH awarded to G.J.B. and J.J.M. as coprincipal investigators. Conflict avoidance for G.J.B. is reviewed and managed by Massachusetts General/Brigham hospitals and for J.J.M. by Harvard Medical School in accordance with the conflict of interest policies of these institutions.

[1]To whom correspondence may be addressed. Email: john_mekalanos@hms.harvard.edu or gjbrenner@mgh.harvard.edu.

This article contains supporting information online at http://www.pnas.org/lookup/suppl/doi:10.1073/pnas.2202719119/-/DCSupplemental.

Published June 8, 2022.

of cancer cells and the use of intravenous (i.v.) delivery. Toxicity limits the size of bacterial inoculum that can be delivered systemically, so patients in i.v. trials may have received doses insufficient to generate bacterial colonization of tumors (17). The only BCT approved by the US Food and Drug Administration involves a live attenuated strain of *Mycobacterium bovis*. For four decades, it has been the standard of care for high-risk non–muscle-invasive bladder cancer (19). To our knowledge, researchers have never tested bacterial therapy for slow-growing benign tumors, such as schwannomas.

Bacterial therapy may be well suited for schwannomas given that they are genetically stable, slow growing, and highly vascularized with hypoxic areas. Thus, schwannomas provide an ideal environment for bacterial homing (20) and survival and a promising target for bacterially mediated tumor cytotoxic and anti-angiogenic effects. Furthermore, schwannomas contain immunosuppressive type 2 macrophages and regulatory T cells (Tregs) (21), providing the immunological milieu that bacterial immune modulators (e.g., lipopolysaccharide, muramyl dipeptide, and cyclic dinucleotides) might alter in ways that help the development of host antitumor immunity. Because some schwannomas are infiltrated with $CD4^+$ and $CD8^+$ T cells that express programmed death-1 receptor (PD-1), it is also likely that anticheckpoint blockade strategies might provide additional enhancement of antischwannoma immune responses (22).

Here, we report a clear therapeutic effect for an attenuated strain of the gram-negative bacterium *S. typhimurium*, VNP20009, in two schwannoma models in mice when live bacterial cells are injected into peripheral tumors. Treatment of tumors also induced measurable therapeutic effects on distal, uninjected tumors and newly implanted tumors, suggesting that antitumor memory immune responses were induced. We also provide evidence that intratumoral (i.t.) bacterial treatment in combination with anti–PD-1 checkpoint inhibition enhances the therapeutic effects observed in the murine schwannoma model we evaluated. Because VNP20009 has been safely administered to patients with metastatic melanoma, renal cell carcinoma, and other malignancies (17, 23), the use of this strain to treat benign schwannoma represents a promising clinical opportunity for future evaluation.

Results

i.t. Injection of Attenuated *S. typhimurium* Suppressed Tumor Growth in Human Xenograft and Murine Syngeneic Schwannoma Models. We performed six independent experiments to assess effects of attenuated *S. typhimurium* on schwannomas and host immune responses. We generated human (HEI-193 cell line) and murine (08031-9 cell line) schwannoma tumors that developed in the sciatic nerves of athymic nude (nu/nu) immunocompromised and syngeneic immunocompetent (FVB/N) mice, respectively (24, 25) and tested two different attenuated strains of *S. typhimurium* (VNP20009 and ΔppGpp) for their therapeutic effects. VNP20009 expresses a modified lipid A to minimize its ability to induce septic shock and is also a purine auxotroph that is reported to augment its growth in the tumor microenvironment and thus enhance tumor targeting (26). Collectively, these mutations increase the median lethal dose (LD_{50}) by 10,000-fold compared with the wild-type *S. typhimurium* (27). The ΔppGpp strain is defective in guanosine 5-diphosphate-3-diphosphate synthesis, resulting in 100,000- to 1,000,000-fold increase in the LD_{50} compared with the wild-type strain (28). Both strains showed high tumor tropism and good safety profiles in preclinical studies (10, 26), and VNP20009 showed a remarkably good safety profile in early clinical studies (17, 23).

We assessed intrasciatic schwannoma burden via in vivo bioluminescence imaging of firefly luciferase (Fluc) expressed by HEI-193FC (human-NF2 schwannoma line) and 08031–9FC (murine *NF2*-deficient schwannoma line) cells (24, 25). Once the tumor signals stabilized (about 2 wk after implanting HEI-193FC or 1 wk after implanting 08031–9FC cells) (Fig. 1 *A* and *B*), we injected tumor-bearing sciatic nerves under direct visualization with $\sim 10^4$ colony-forming units (CFUs) of attenuated *S. typhimurium* cells (either VNP20009 or ΔppGpp) or phosphate-buffered saline (PBS) control. Tumor growth was assessed over the subsequent 5 wk in the human xenograft nude mice and subsequent 2 wk in the syngeneic immunocompetent mice. The study in syngeneic mice was terminated at 18 d after implanting tumor cells because control mice developed motor dysfunction of the tumor-bearing hind limb (as assessed by coauthor S.G.A. and an animal care technician, who were blinded to group assignment). We replicated this study twice in the xenograft and once in the syngeneic model (*SI Appendix*, Fig. S1).

In all three replicates in the xenograft schwannoma model, VNP20009 decreased tumor signal compared with PBS control (Fig. 1*A* and *SI Appendix*, Fig. S1*A*). Approximately 75% of the VNP20009-injected tumors in xenograft mice had no bioluminescent signal at the time of study termination. In both replicates using the syngeneic model, VNP20009 reduced tumor growth about eightfold relative to PBS (Fig. 1*B* and *SI Appendix*, Fig. S1*B*). VNP20009 regressed the tumor signal to undetectable levels in five of eight syngeneic-tumor mice (Fig. 1*B*). Tumor growth curves for VNP20009- and PBS-injected mice diverged in both tumor models as early as 1 wk after i.t. injection. The effect of the ΔppGpp strain on tumor volume in xenograft mice was indistinguishable from that of VNP20009. In syngeneic mice, ΔppGpp did not reduce tumor growth compared with PBS; in contrast, VNP20009 controlled growth significantly better than the ΔppGpp strain (Fig. 1*B*).

In both tumor models, tumor-bearing nerves harvested at the end of the experiment had abundant apoptotic bodies in both VNP20009- and ΔppGpp-injected tumors, while tumors injected with PBS had very few or no apoptotic bodies (Fig. 1 *C* and *D*). Apoptotic bodies were approximately three times more prevalent in VNP20009-injected tumors than in ΔppGpp-injected tumors.

***S. typhimurium* Induced Proimmunogenic Cytokines, Immune Cell Infiltration, and Inflammasome Proteins in the Syngeneic Schwannoma Model.** To assess parameters related to the host antitumor immune response, we killed syngeneic mice just prior to significant morbidity in treated and control animals (approximately 2 wk after bacterial or PBS injection) and harvested samples for analysis by fluorescence-activated cell sorter. In xenograft mice, samples were harvested after the resolution of tumor signal in most animals (approximately 5 wk after bacterial/PBS injection). At the time of sacrifice, both strains of *S. typhimurium* increased $CD45^+$ (leukocytes) and $CD68^+$ (predominantly macrophages) cellular infiltration significantly compared with PBS-injected tumors in syngeneic and human xenograft mice (Fig. 2 *A* and *B* and *SI Appendix*, Fig. S2). Thus, i.t. injection of VNP20009 and ΔppGpp induced indicators of innate and adaptive immune responses in mouse schwannomas in syngeneic immunocompetent mice, as well as innate responses in human schwannomas in nude mice.

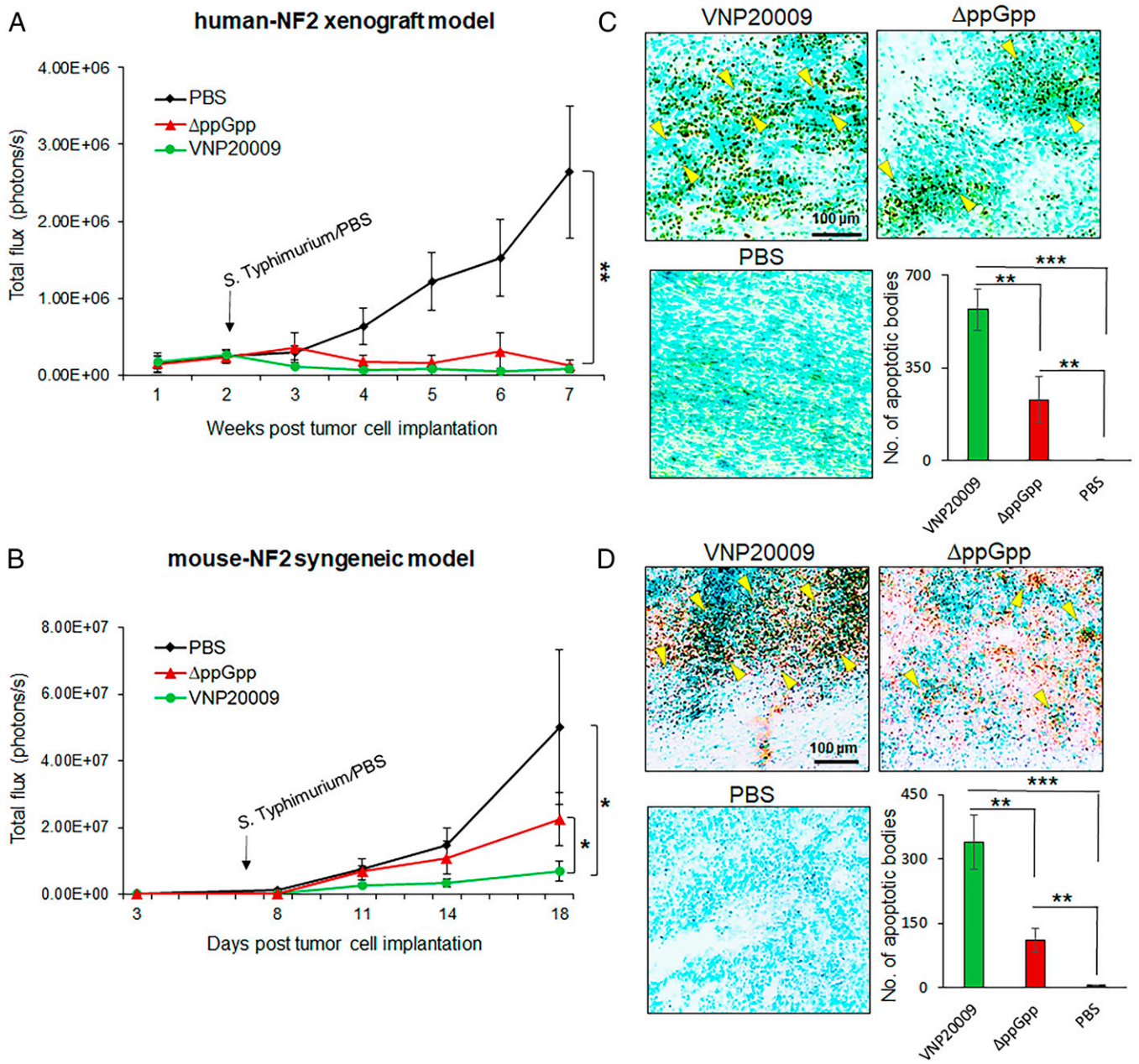

Fig. 1. i.t. injection of attenuated *S. typhimurium*–controlled schwannoma development in human xenograft and syngeneic schwannoma models. (*A* and *B*) Volume of tumors over time by treatment in (*A*) xenograft mice and (*B*) syngeneic mice (n = 8 mice/group). (*C* and *D*) i.t. VNP20009 and ΔppGpp increased apoptosis in both the human xenograft (*C*) and syngeneic (*D*) mice compared with PBS (n = 3 mice/group; yellow arrowheads indicate representative apoptotic cells). Repeated-measures ANOVA with Bonferroni post hoc test was used to compare tumor signals between groups and between pre- and postbacterial injection, and one-way ANOVA was used for analysis of apoptosis. Data are shown as mean ± SEM. *P < 0.05, **P < 0.01, ***P < 0.00.

We focused our further investigation on the immunogenic cellular and cell death responses in the syngeneic immunocompetent mice. A key determinant of host antitumor immunity is the balance of i.t. M1 (tumoricidal) (29) and M2 (tumorigenic) (30) macrophages (31). i.t. injection of VNP20009, relative to PBS, shifted the balance significantly toward M1-type macrophages at 3 d after injection, a change that became even more pronounced at 7 d after injection (Fig. 2*C*). However, i.t. injection of ΔppGpp, compared with PBS, shifted the balance only temporarily, with the effect at 3 d after injection disappearing by 7 d after injection. Both *S. typhimurium* strains had systemic effects, resulting in more splenic macrophages ($CD45^+$ $F4/80^+$) 3 d after i.t. injection than for PBS (*SI Appendix*, Fig. S3*A*). Moreover, neutrophil infiltration of schwannomas was increased by VNP20009 and by ΔppGpp compared with PBS as assessed 7 d after i.t. injection of the bacteria (*SI Appendix*, Fig. S3*B*).

We also investigated whether i.t injection of attenuated *S. typhimurium* influenced the i.t. T cell composition and the levels of immunostimulatory cytokines that regulate the survival, proliferation, and differentiation of both immune and tumor cells (32–34). Both bacterial strains, relative to PBS, boosted the proportions of tumor-infiltrating cytotoxic T cells ($CD3^+$/$CD8^+$) and reduced the proportion of Tregs ($CD4^+$/$CD25^+$) but did not affect helper T cells ($CD3^+$/$CD4^+$) (Fig. 2*D*). In intrasciatic schwannomas, transcript levels of the proinflammatory cytokines tumor necrosis factor–α, interferon-γ, interleukin (IL)-1β, and IL-18 were significantly more up-regulated in

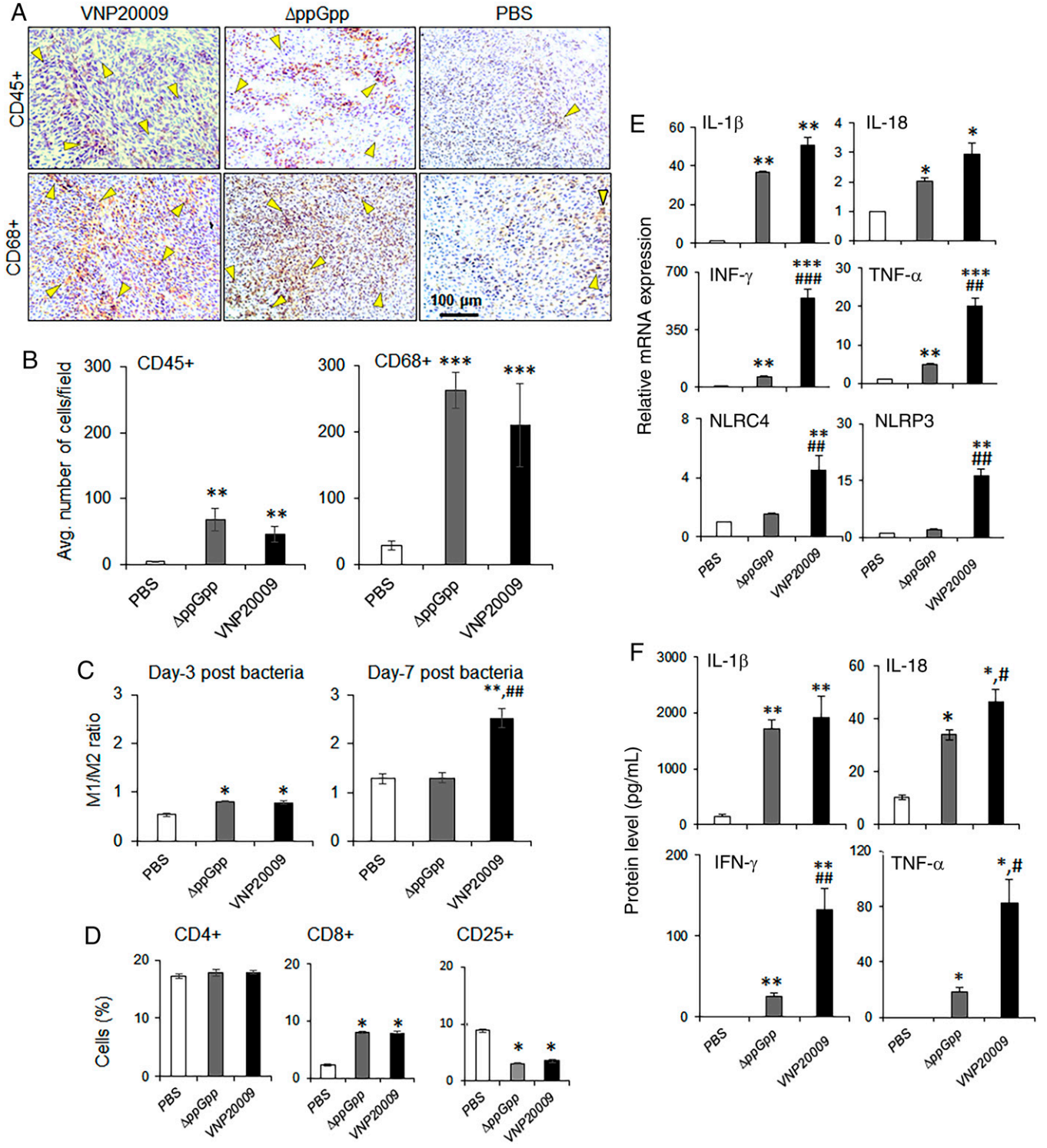

Fig. 2. i.t. *S. typhimurium* increased immune cell infiltration and proinflammatory cytokines in intrasciatic schwannomas in syngeneic mice. (*A*) Yellow arrowheads indicate positive staining of infiltrated immune cells ($CD45^+$ common leukocytes and $CD68^+$ pan macrophages). (*B*) Quantified levels of infiltrated immune cells by i.t. treatment. (*C* and *D*) Flow cytometric analyses of the $CD45^+$ $F4/80^+$ tumor-associated macrophages and lymphocytes. (*C*) Ratios of M1 ($CD86^+$) to M2 ($CD206^+$) macrophages at 3 and 7 d after i.t. treatment. (*D*) i.t. T cell populations at 7 d after bacterial/control injection. Percentages represent proportions of $CD45^+$ cells. *SI Appendix*, Fig. S8 shows flow cytometric profiles. (*E* and *F*) i.t. transcript levels of inflammatory cytokines and inflammasomes from qRT-PCR (*E*) and corresponding cytokine protein levels from enzyme-linked immunosorbent assay (*F*) 3 d after bacterial/control injection. $n = 3$ mice per group for all results. One-way ANOVA used to compare between the different treatments. Data are shown as mean ± SEM. Asterisks (*) denote differences with PBS control; hash signs (#) denote differences with ΔppGpp. */# $P < 0.05$, **/## $P < 0.01$, ***/### $P < 0.001$. Avg., average; IFN, interferon; TNF, tumor necrosis factor.

response to the *S. typhimurium* strains than to PBS 3 d after i.t. injection, with VNP20009 generally eliciting significantly stronger effects than ΔppGpp (Fig. 2*E*). Differences in the levels of cytokine proteins across i.t. bacterial treatments (Fig. 2*F*) corresponded with the differences in their respective cytokine transcript levels. VNP20009 also produced significantly more messenger RNA (mRNA) for components of the NLRC4 and NLRP3 inflammasomes than ΔppGpp or PBS (Fig. 2*E*).

However, i.t. injection of *S. typhimurium* did not alter serum cytokine levels (*SI Appendix*, Fig. S4).

Finally, we used standard gentamicin invasion assays to measure the ability of both *S. typhimurium* strains to invade relevant mammalian cell lines. We found that in cocultures with either macrophage or schwannoma cell lines, VNP20009 was more invasive than ΔppGpp but less invasive than its parent type *S. typhimurium* 14028s (*SI Appendix*, Fig. S5). Furthermore, macrophages released inflammatory cytokines after coculture with the attenuated *S. typhimurium* strains, but schwannoma cell lines cocultured with the same bacterial strains did not (*SI Appendix*, Figs. S6 and S7).

Combination of i.t. Injection of *S. typhimurium* VNP20009 and Systemic PD-1 Monoclonal Antibody (mAb) Induced a Potent Systemic Immune Response Against Subcutaneous (s.c.) Schwannomas in Syngeneic Mice. High PD-1 expression in human schwannomas indicates resistance to cell-mediated immunity in the tumor immune microenvironment (22). We evaluated whether adding systemic anti–PD-1 mAb therapy enhanced the apparent antitumor adaptive immune responses stimulated by i.t. injection of VNP20009. We implanted 08031–9 mouse schwannoma cells s.c. into both flanks in syngeneic mice, dividing them into four groups: i) i.t. VNP20009 only (left flank tumor); ii) intraperitoneal (i.p.) anti–PD-1 mAb only; iii) i.t. VNP20009 (left flank tumor) and i.p. anti–PD-1 mAb; and iv) i.t. PBS only (left flank tumor) (Fig. 3*A*). s.c. implantation allowed longer survival than intrasciatic implantation, giving more opportunity for adaptive immune responses to occur. Once mean tumor size reached ∼150 mm^3 (35) (11 d after implantation), we injected 10^4 CFUs in PBS or PBS only directly into left flank tumors. Anti–PD-1 mAb was administered i.p. (250 μg/injection) on days 10 (one day before VNP20009 injection), 13, 16, and 19 after implanting schwannoma cells (36). VNP20009 alone, anti–PD-1 mAb, and combination therapy each suppressed growth of tumors in both flanks relative to PBS (Fig. 3 *B* and *D*). Combination therapy was more effective than either therapy alone for injected tumors and was more effective than anti–PD-1 mAb alone for uninjected contralateral tumors. Also, VNP20009 controlled growth significantly better than anti–PD-1 mAb alone in the uninjected, but not the injected, tumors. In the injected tumors, VNP20009 and anti–PD-1 mAb monotherapies performed similarly, increasing $CD8^+$ cytotoxic T ($CD3^+/CD8^+$) cells and $CD4^+$ helper T ($CD3^+/CD4^+$) cells and decreasing $CD25^+$ regulatory T ($CD4^+/CD25^+$) cells compared with PBS (Fig. 3*C*). Combination therapy had additive improvements over the monotherapies. Systemic host antitumor immune responses to the different treatments relative to uninjected tumors were broadly similar when measured by immune effector cell type abundance (Fig. 3*E*).

Combination of i.t. Injection of *S. typhimurium* VNP20009 and Systemic Anti–PD-1 mAb Induced a Potent, Protective, and Systemic Immune Response Against Subsequent Orthotopic Schwannoma Rechallenge. Next, we investigated whether i.t. injection of VNP20009 alone or in combination with anti–PD-1 mAb generated a lasting systemic antitumor adaptive immune response in an orthotopic tumor rechallenge model. For the first part of this experiment, we used mostly the same procedures and design as in the immediately prior experiment. The differences were that we injected mice i.t. with bacteria/PBS control treatments 8 d after implanting schwannoma cells and injected anti–PD-1 mAb i.p. (250 μg/injection) (36) on days 7, 10, 13, and 16 after implanting schwannoma cells. The results for the injected tumor from this experiment mirror those from the previous one (Fig. 4 *B* and *C*). Twenty days after implanting schwannoma cells s.c. into left flanks, we rechallenged mice orthotopically by implanting mouse schwannoma cells into their contralateral sciatic nerves. Preimplantation VNP20009 monotherapy and combination therapy both strongly controlled growth in rechallenge intrasciatic tumors compared with PBS (Fig. 4*D*). Anti–PD-1 mAb monotherapy did not control rechallenge intrasciatic tumor growth significantly better than PBS. VNP20009's suppressive effect on the rechallenge intrasciatic tumors appears even greater than that on the injected s.c. tumors (Fig. 4 *B* and *D*). Moreover, VNP20009 monotherapy's and combination therapy's effects on T cell composition were very similar for rechallenge intrasciatic tumors and primary injected s.c. tumors (Fig. 4 *C* and *E*); that is, these treatments increased $CD4^+$ helper and $CD8^+$ cytotoxic cells and decreased $CD25^+$ Treg cells relative to PBS.

We further examined whether there was viable *S. typhimurium* in i.t. VNP20009-injected s.c. tumors, uninjected contralateral s.c. tumors, and rechallenge intrasciatic tumors. We cultured *S. typhimurium* from injected s.c. tumors at all testing time points (1, 3, 7, and 14 d after bacterial injection) but were unsuccessful in culturing *S. typhimurium* from uninjected contralateral s.c. tumors at any time point (*SI Appendix*, Fig. S10*A*). In addition, we performed a more sensitive assay on tumor homogenates from mice at the time of sacrifice from this and the prior experiment. We detected expression of VNP20009 aroC mRNA only in the injected s.c. tumors but not in the uninjected contralateral s.c. or rechallenge intrasciatic tumors (*SI Appendix*, Fig. S10 *B* and *C*). Thus, it is exceptionally unlikely that VNP20009's suppressive effect on uninjected contralateral s.c. tumors (Fig. 3) and rechallenge intrasciatic tumors was due to *S. typhimurium* colonizing these untreated distal or newly established tumors.

i.t. Attenuated *S. typhimurium*–Suppressed Schwannoma Angiogenesis in Syngeneic Mice. Immune cells, including tumor macrophages and $CD25^+$ Tregs, interact with tumor cells, inducing angiogenesis and suppressing antitumor immunity. Vascular endothelial growth factor (VEGF) and PD-1 are critical for these host–tumor cell–cell interactions (37). Tumor hypoxia and angiogenesis promote infiltration of tumorigenic M2-type macrophages (38), which themselves stimulate angiogenesis and suppress antitumor immunity (39). Hypoxia, angiogenesis, and abundant tumor-promoting macrophages are hallmarks of schwannomas. Bevacizumab, an anti-angiogenic mAb directed against VEGF-A, can control schwannoma growth in a subset of individuals with schwannoma (40). *S. typhimurium* also reduces expression of VEGF and has had anti-angiogenic properties in preclinical cancer models (14). Therefore, we assessed the effect of i.t. injection of attenuated *S. typhimurium* on tumor vascularity in syngeneic mice. Compared with PBS, both VNP20009 and ΔppGpp strains inhibited angiogenesis in intrasciatic tumor tissues harvested 2 wk after i.t. injection, as indicated by direct visualization and immunohistochemistry for the vascular endothelial marker CD31 (41) (Fig. 5).

Motility and Adhesion to Mammalian Cells Affect the Antitumor Properties of *S. typhimurium* VNP20009. To better understand the mechanisms underlying the antischwannoma therapeutic effect of VNP20009, we carried out a phenotypic and genotypic characterization of the strain. Examination of the growth of VNP20009 and its 14028s parental strain culture in soft agar and by light microscopy in wet mounts revealed that VNP20009 was neither motile nor chemotactic (Fig. 6*A*).

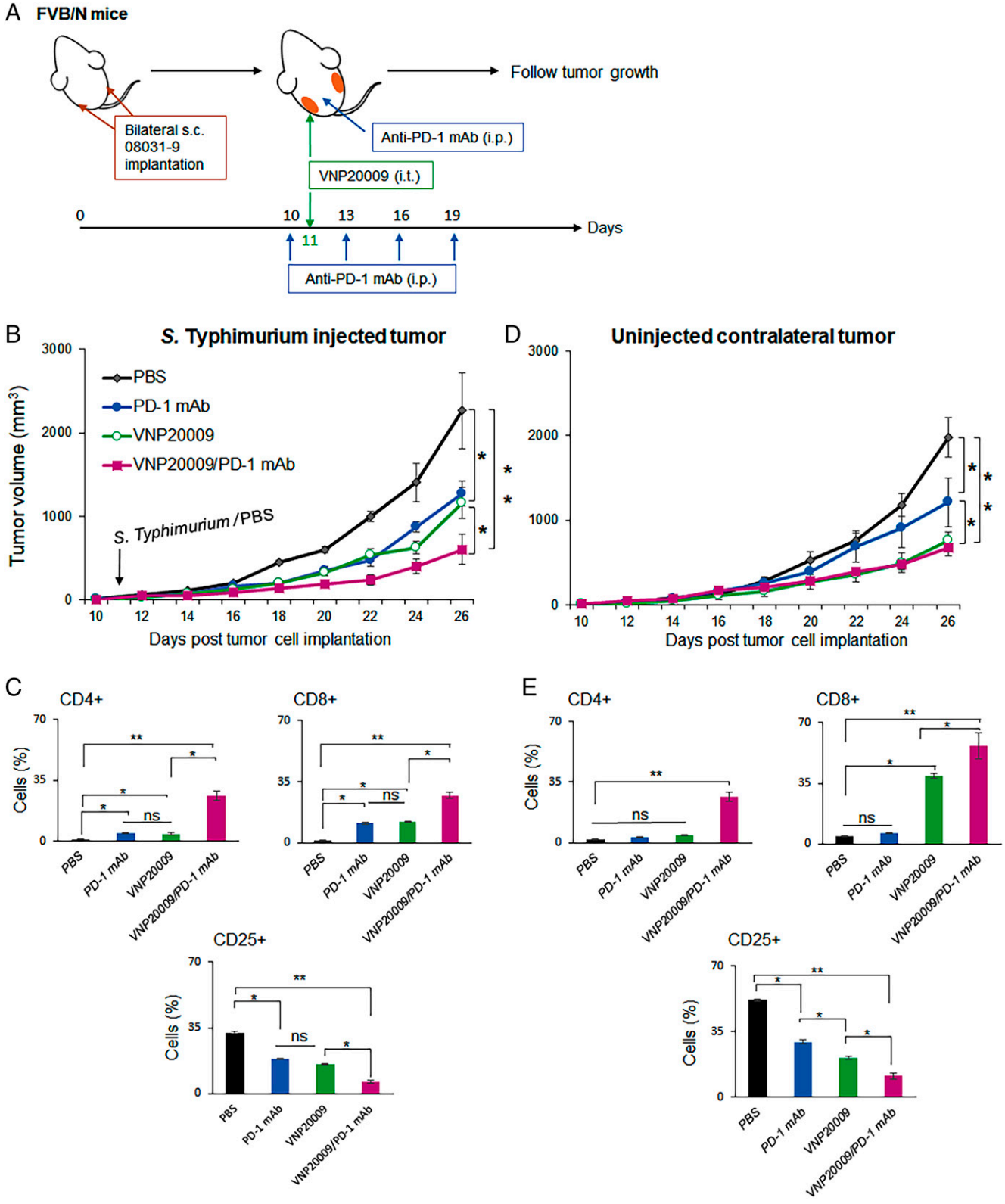

Fig. 3. i.t. VNP20009 inhibited growth of injected and uninjected distal schwannomas, and i.p. anti–PD-1 mAb enhanced the effects in syngeneic mice. (*A*) Schematic of the experimental design. (*B*) Volume of injected tumors over time by treatment (n = 6 mice/group). (*C*) T cell composition in injected tumors harvested 26 d after implantation (n = 3 mice/group). (*D*) Volume of contralateral uninjected tumors over time by treatment (n = 6 mice/group). (*E*) T cell composition in uninjected tumors harvested 26 d after implantation (n = 3 mice/group). *SI Appendix*, Fig. S9 shows the flow cytometric profiles. Repeated-measures ANOVA was utilized to compare the tumor volumes between the different groups, and one-way ANOVA was used to compare the flow cytometric quantification. Data are shown as mean ± SEM. *P < 0.05, **P < 0.01. ns, not significant.

Interestingly, the impaired motility of VNP20009 appears not due to defects in flagellin synthesis, export, or assembly, as suggested by the levels of the major expressed flagellin filament protein FliC (*SI Appendix*, Fig. S12*A*). FliC was secreted and appeared polymerized when observed by electron microscopy (Fig. 6*B*). Through whole genomic sequencing and Single

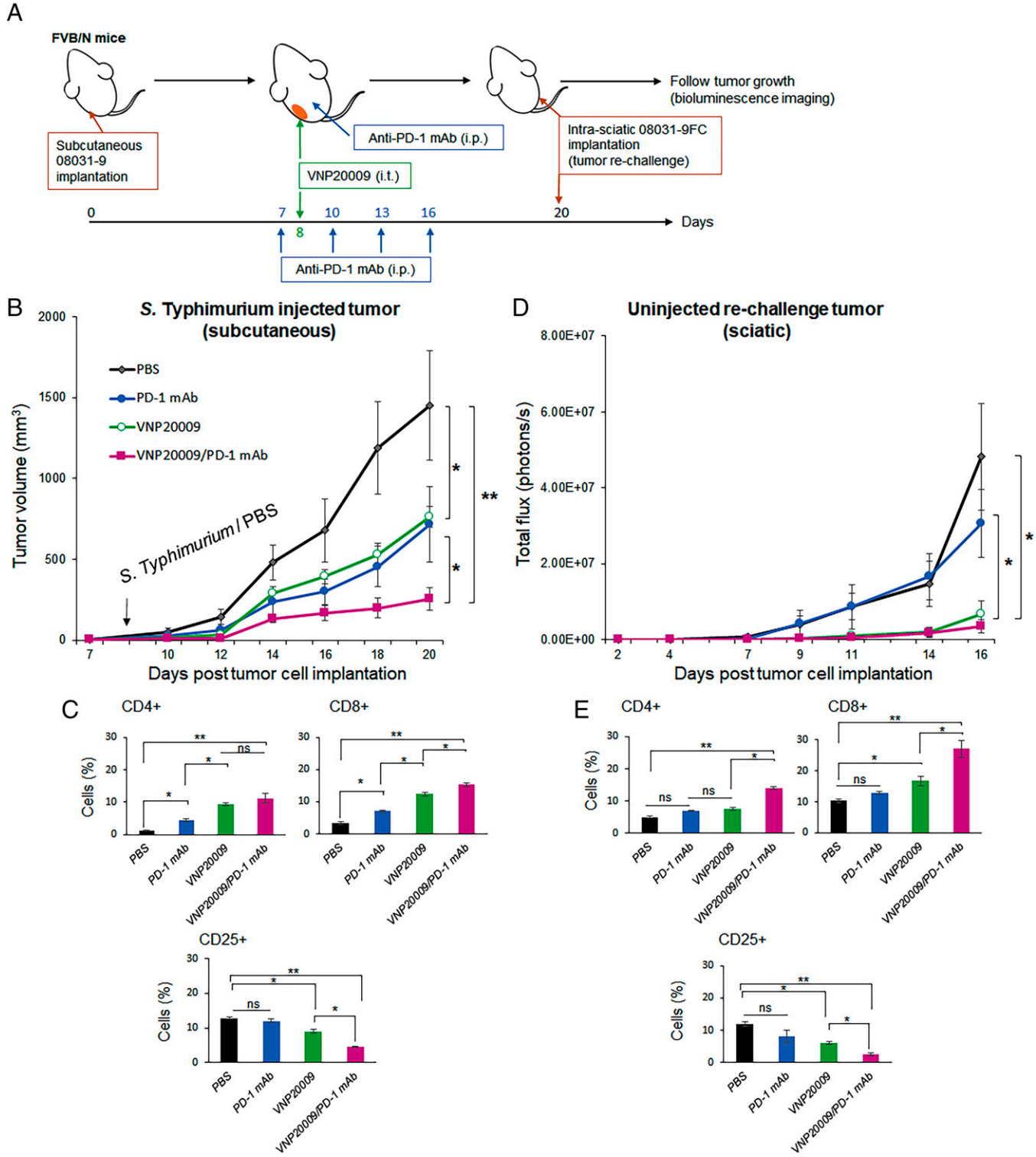

Fig. 4. i.t. VNP20009 inhibited tumor growth of injected s.c. and subsequently implanted rechallenge intrasciatic schwannomas in syngeneic mice. (*A*) Schematic of the experimental design. (*B*) Volume of injected s.c. tumors over time by treatment (n = 6 mice/group). (*C*) T cell composition in injected s.c. tumors harvested at the end of the study (n = 3 mice/group). (*D*) Volume of rechallenge intrasciatic tumors over time by treatment (n = 6 mice/group). (*E*) T cell composition in rechallenge intrasciatic tumors harvested 16 d after implantation (n = 3 mice/group). *SI Appendix*, Fig. S11 shows the flow cytometric profiles. Repeated-measures ANOVA was utilized to compare the tumor volumes and bioluminescence between the different groups, and one-way ANOVA was used to compare the flow cytometric quantification. Data are shown as mean ± SEM. *P < 0.05, **P < 0.01. ns, not significant.

Nucleotide Variant (SNV) analysis, we identified ~90 SNVs between VNP200009 and its parental strain, 14028s (Table S1). One of these SNVs is located in *fliF*, a gene essential for flagellar function, and this mutation could explain why VNP20009 is not motile. To further characterize this VNP20009 phenotype, we isolated a spontaneous motile VNP20009 variant (named Mot+) and defined its genetic changes by whole genome sequencing. This analysis demonstrated SNVs in both the *fliM* gene, which encodes the flagellar motor switch protein FliM, and in the *rcsB* gene, which encodes a transcriptional regulator of flagellar and

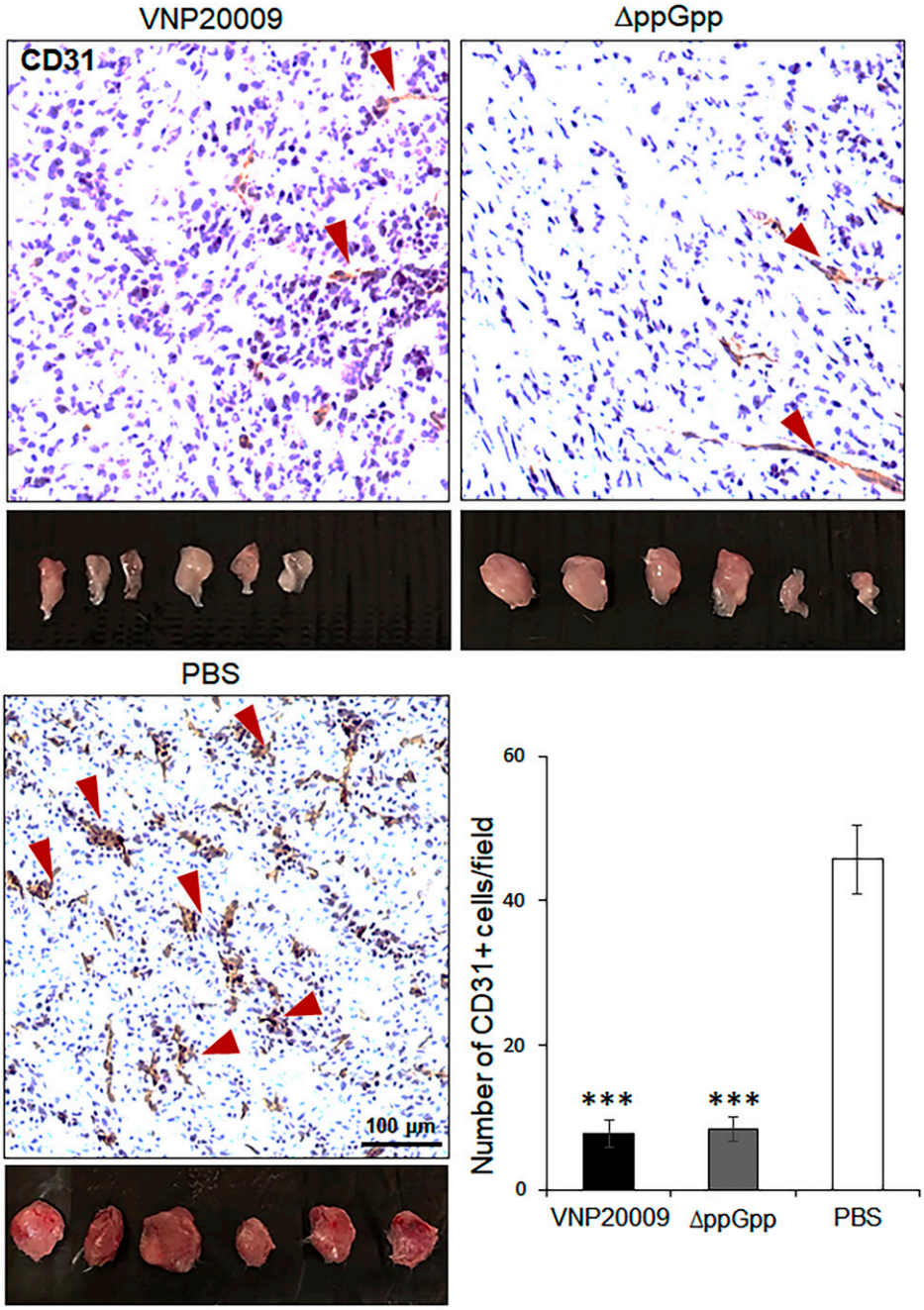

Fig. 5. i.t. attenuated *S. typhimurium* inhibited angiogenesis in intrasciatic schwannomas in syngeneic mice. Tumors injected with PBS (n = 6 mice, *Lower left*) were bright red and had prominent external vascularity. In contrast, tumors injected with VNP20009 (n = 6 mice, *Upper left*) and ΔppGpp (n = 6, *Upper right*) were pale in color with little or no external vascularization. VNP20009 and ΔppGpp reduced the number of infiltrating $CD31^+$ cells (*Lower right*; also indicated by red arrowheads in micrographs of representative staining; n = 3 mice/group). One-way ANOVA was utilized for quantification analysis. Data are shown as mean ± SEM. ***$P < 0.001$.

virulence genes. These two SNVs might explain the restoration of motility in the Mot+ strain through, presumably, suppression of the mutation in *fliF* or another SNV present in VNP20009 that affects its motility and chemotaxis properties.

To investigate whether regaining motility and chemotaxis alters the efficacy of VNP20009 as an anti-NF2 tumor therapy, we compared the growth of s.c. 08031–9 mouse schwannomas following i.t. injection with VNP20009, Mot+, and PBS. Once mean tumor size reached ∼150 mm^3 (35) (12 d after implantation), we injected 10^4 CFUs of bacteria in 100 μL or PBS directly into left flank tumors. As expected, VNP20009 controlled tumor growth compared with PBS but, surprisingly, there was no effect on schwannoma growth after i.t. injection of Mot+ (Fig. 6*C*). We then determined the transcriptome of Mot+ and VNP20009 growing exponentially in rich media by RNA sequencing (RNA-seq) (Fig. 6*D*). Compared with VNP20009, Mot+ expressed higher levels of transcripts corresponding to the FliC gene encoding flagellin, a well-known innate immune agonist (42). However, Mot+ showed that down-regulation of genes involved the expression of Type I fimbriae, which are bacterial organelles that mediate cellular adhesion; this RNA-seq finding was confirmed by qPCR analysis (*SI Appendix*, Fig. S12*B*). Furthermore, SNV analysis of VNP20009 revealed a point mutation located in the *fimH* gene (encoding a transcriptional regulator of Type I fimbrial expression). These results suggest that cellular adhesion might affect the antitumor properties of VNP20009.

To assess whether our bacterial transcriptomic data had phenotypic correlations, we performed in vitro adhesion and invasion assays utilizing the 08031–9 mouse schwannoma cell line. Mot+ showed a drastic decrease of adhesion to schwannoma cells compared with both VNP20009 and parental 14028s (Fig. 6*E*). However, we observed no difference between the two strains in their ability to invade and survive intracellularly

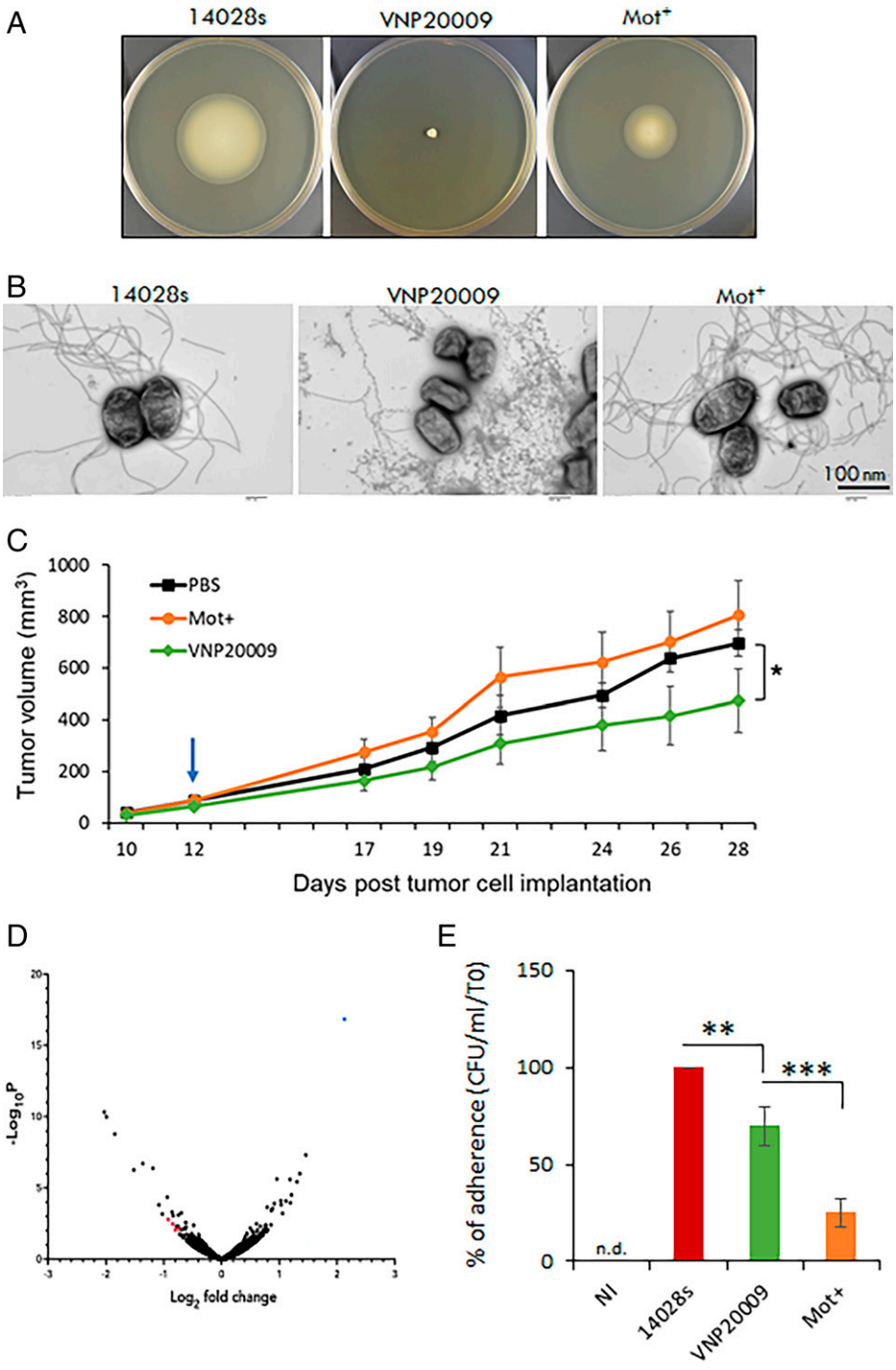

Fig. 6. *S. typhimurium* VNP20009 motility is associated with lack of schwannoma growth control. (*A*) Motility assay on agar plates following inoculation with 14028s (VNP20009 parental strain), VNP20009, and the motile derivative of VNP20009, Mot+ (performed on Luria broth containing 0.3% [W/V] agar). (*B*) Electron microscopic images of 14028s, VNP20009, and the Mot+. (*C*) i.t. VNP20009 but not Mot+ controlled growth of s.c. mouse schwannomas (n = 8 mice/group); blue arrow shows time of i.t. injection (day 12 after tumor cell implantation). (*D*) Volcano plot representing the transcriptome profiles comparing Mot+ and VNP20009. The blue dot depicts greater expression of *fliC* in Mot+, whereas the red dots indicate down-regulated fimbriae genes (n = 3/strain). (*E*) Assessment of adhesion of *S. typhimurium* 14028s, VNP20009, and Mot+ to the mouse schwannoma cell line, 08031–9 (n = 3 replicates). n.d., not detectable; NI, not infected. Data are shown as mean ± SEM. Repeated-measures ANOVA was utilized to compare the tumor volumes between the different groups (*C*), and one-way ANOVA was used for analysis of adhesion (*E*). $^{*}P < 0.05$, $^{**}P < 0.01$, $^{***}P < 0.001$.

within schwannoma 08031–9 cells (*SI Appendix*, Fig. S12 *C* and *D*). In contrast, compared with VNP20009, Mot+ bacteria were less capable of invading and/or surviving inside RAW 264.7 macrophages. While this result suggests that Mot+ may be less able to withstand macrophage killing within the tumor microenvironment, we acknowledge that further work will be needed to understand which in vitro bacterial properties correlate best with antitumor efficacy in these preclinical mouse models.

***S. typhimurium* Suppresses Growth of s.c. Human Malignant Peripheral Nerve Sheath Tumors (MPNSTs) and Human Meningiomas in Xenograft Mouse Models.** We also evaluated the effect of i.t. injection of VNP20009 and ΔppGpp on human MPNSTs and meningiomas in xenograft mice. These NF1- and NF2-associated tumors grow relatively slowly and therefore have this property in common with NF2-associated benign schwannomas. In separate sets of animals, we implanted NF1-associated MPNST (S462TY; Fig. 7*A*) (43), sporadic MPNST (STS26T; Fig. 7*B*) (44), benign meningioma (Ben-Men-1; Fig. 7*C*), and malignant meningioma (CH-157 MN; Fig. 7*D*) cells (45), s.c. in left flanks. In each xenograft model, we injected VNP20009 (10^4 CFUs in 100 μL), ΔppGpp (10^4 CFUs in 100 μL), or PBS i.t. after tumor volume had reached ~150 mm^3. The lengths of the experiment varied from 23 to 41 d across models because of variation in speed of initial pretreatment tumor growth and development of complications in control mice. VNP20009 and ΔppGpp suppressed growth of tumors dramatically better than PBS in all xenograft models

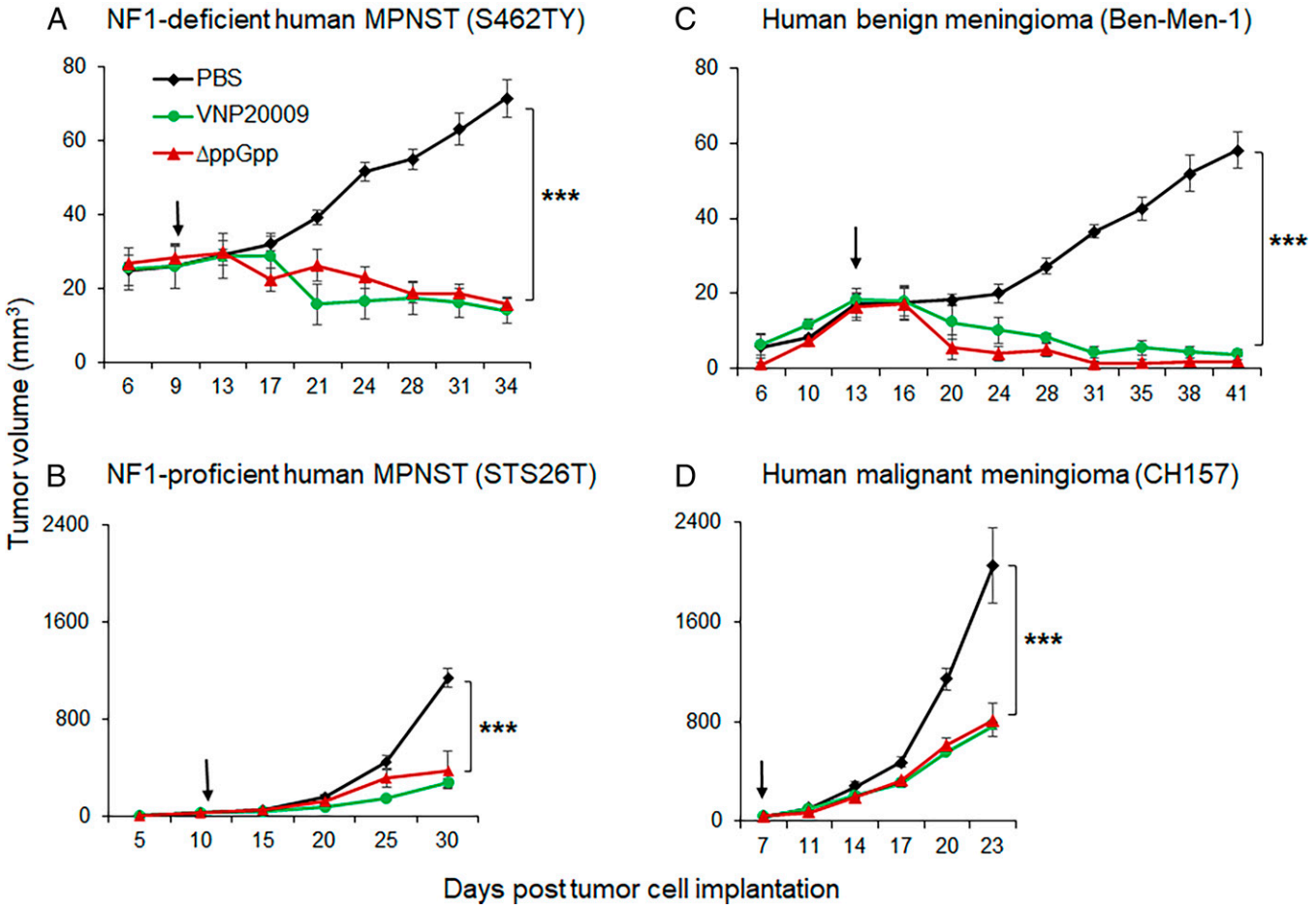

Fig. 7. i.t. injection of two *S. typhimurium* strains suppressed growth of human MPNSTs and meningiomas in xenograft mice. (*A–D*) Tumor volume by treatment group in xenograft mice with (*A*) NF1-associated MPNSTs, (*B*) sporadic MPNSTs, (*C*) benign meningiomas, and (*D*) malignant meningiomas. Arrows indicate time of i.t. injection. $n = 5$ mice/group. Repeated-measures ANOVA with Bonferroni post hoc test was used to compare tumor volume between groups and between pre- and postbacterial injection. Data are shown as mean ± SEM. ***$P < 0.001$.

(Fig. 7). For NF1-associated nerve sheath tumors and benign meningiomas, attenuated *S. typhimurium* strains caused tumor regression completely in two of five meningioma xenograft mice for each strain (Fig. 7 *A* and *C*). For sporadic MPNST and malignant meningioma, there was an approximate threefold reduction in the tumor size in mice injected with the *S. typhimurium* strains compared with the PBS control. These results suggest that attenuated strains such as VNP20009 and ΔppGpp may represent promising therapeutics for treatment of benign and malignant neoplasms if they are relatively slow growing as well as immunologically and metabolically similar to schwannoma.

Discussion

In a series of experiments, we evaluated bacterial treatment of schwannoma and related benign and malignant neoplasms. i.t. injection of live *S. typhimurium* bacterial cells of two different attenuated strains controlled the growth of intrasciatic benign schwannoma in human xenograft and mouse syngeneic models. The VNP20009 strain controlled growth significantly in both models, usually eliminating tumors entirely in the xenograft model. The ΔppGpp strain inhibited growth in the human xenograft model but not the syngeneic mouse schwannoma model. While the mechanisms underlying this difference in efficacy are not well understood, both strains increased infiltration of immune cells into tumors, shifted the balance of resident macrophages from the tumorigenic M2 type to the tumoricidal M1 type, and inhibited angiogenesis in tumors. VNP20009 was more effective than ΔppGpp in invading tumor cells in vitro, eliciting proimmunogenic cytokines and inflammasome proteins and inducing tumor cell apoptosis.

VNP20009 controlled the growth of uninjected contralateral s.c. schwannomas and rechallenge intrasciatic schwannomas (i.e., implanted after injection of VNP20009 in the primary tumor). These results suggest that systemic antitumor immunological mechanisms underlie the efficacy seen with attenuated *S. typhimurium* strains when used in these therapeutic disease models. Our findings and interpretation are consistent with the vaccination-like effects of other BCTs seen in previous studies, which include induction of tumor-targeted T helper type 1 (Th1)-mediated cytotoxic responses (13, 46, 47). Furthermore, both VNP20009 and ΔppGpp controlled growth of two neoplasms, one a schwannoma associated with NF2 disease and the other a meningioma associated with NF1 disease. In all six of the murine tumor models we explored, we found that the *S. typhimurium* strains tested controlled tumor growth best when tumors were slow growing. This bodes well for translation to human therapeutic applications because human NF2 schwannomas tend to be very slow growing.

We observed that VNP20009 lacks a functional flagellar apparatus and therefore hypothesized that regaining motility

might enhance its antitumor efficacy by promoting deeper immune activation as a result of enhanced expression of flagellin, a known innate immune agonist of Toll-like receptor 5 (42). For example, compared with its parent, a strain of *S. typhimurium* that was engineered to secrete a heterologous flagellin from *Vibrio vulnificus* has been reported to enhance bacterial tumor killing in a mouse cancer model (11). We were able to isolate a motile derivative of VNP20009, which we named simply Mot+. Contrary to our prediction, strain Mot+ did not demonstrate any antitumor efficacy compared with VNP20009 in our syngeneic mouse 08031–9 s.c. schwannoma model. To gain insight into what caused the loss of motility in VNP20009 and the reduced therapeutic efficacy in control of schwannoma by Mot+, we conducted genome sequencing and RNA-seq analysis of VNP20009, its parental strain 14028s, and strain Mot+. This analysis revealed an SNV in *fliF* in VNP20009 compared with 14028s; however, Mot+ carried different mutations in other flagellar genes that probably resulted in suppression of the motility defect in VNP20009 regardless of whether the *fliF* mutation identified was involved. Furthermore, transcriptome analysis of VNP20009 and Mot+ suggested that an alteration in expression of Type I fimbriae correlated with diminished adhesion of Mot+ (compared with the VNP20009) to the mouse schwannoma cell line 08031–9. Interestingly, we found no difference between Mot+ and VNP20009 in in vitro invasion of 08031–9 tumor cells. However, the Mot+ strain was less capable of invading and surviving in RAW 264.7 macrophages in vitro. Thus, VNP20009 is likely different from the less efficacious motile strain in a variety of properties, and this may include the degree and type of inflammasome induction within macrophages, potentially leading to greater macrophage-mediated killing of the motile strain. It is also possible that the tumor killing efficacy of VNP20009, in contradistinction to the motile strain, may be due in part to bacterial-mediated macrophage activation—with or without bacterial cell entry—in a manner that does not lead to macrophage cell death. This macrophage activation may include inflammasome induction that promotes antitumor immune responses. In support of this hypothesis, *S. typhimurium* is well-known to induce inflammasomes in both murine (48, 49) and human (50–52) macrophages, and more recently, *S. typhimurium* infection was shown to cause rapid stimulation of Th1 responses via pathways involving microbe-associated molecular patterns (53). In a 2022 publication, Mónaco and coinvestigators (54) demonstrated that both macrophages and inflammasome activation play an essential role in murine modeling of *Salmonella* therapy of melanoma. Our findings in conjunction with published data support the conclusion that VNP20009 entry and survival in macrophages in vivo may be a critical step in its control of schwannoma growth. If so, does successful bacterial tumor therapy in this case reflect bacterial persistence within the tumor through resisting macrophage killing or altering macrophage activation? This complex question remains to be answered in future studies that will include bacterial mutant analysis designed to alter properties associated with invasion and survival of *S. typhimurium* within macrophages.

In our syngeneic murine schwannoma model, combining systemic PD-1 immune checkpoint inhibition with VNP20009 treatment improved antitumor efficacy over VNP20009 alone for injected primary s.c. tumors but not uninjected contralateral or rechallenge intrasciatic tumors, despite enhancing immune responses in all tumors. A possible explanation for this may be the vastly fewer tumor cells injected into the sciatic nerve to generate rechallenge tumors than were present in the primary s.c. tumors, where we initiated bacterial treatment. In future experiments, the durability and strength of combination therapy relative to monotherapy might be determined by increasing the observation time after i.t. injection and rechallenge. Also ripe for further study is the impact of PD-1 immune checkpoint inhibition on functional (e.g., effector versus exhausted T cells) and differential (e.g., early memory versus effector memory T cells) status of these tumor-infiltrating lymphocytes. Such investigations may provide insight into the immune mechanisms underlying the therapeutic efficacy we observed and guide an optimized bacteria-based immunotherapeutic strategy for schwannoma.

Our experiments provide preclinical validation of i.t. injection of an attenuated *S. typhimurium* as an immunotherapy for a benign neoplasm. VNP20009 has been studied in human volunteers as an anticancer therapy for disseminated malignant neoplasms. In these human studies, VNP20009 was generally very well-tolerated following both i.v. and i.t. delivery (17, 18). Thus, we anticipate that a phase I study of VNP20009 evaluating its safety after i.t. injection into human schwannomas could proceed without additional toxicity or efficacy studies beyond the murine models described here. Furthermore, although VNP20009 was not efficacious in the control of aggressive disseminated cancers in humans, there are fundamental differences in the biology of benign neoplasms compared with malignant neoplasms that include the former's substantially slower growth rate and their tendency to reside within a cold immunological milieu, which collectively may allow bacterial antitumor therapy to work more effectively in the treatment of benign neoplasms such as those associated with NF2 disease.

Further development of our approach may be quite fruitful. For instance, it may be possible to engineer *S. typhimurium* to deliver checkpoint inhibitors via nanobodies (55) or small interfering RNA (56), thereby avoiding the substantial side effects with systemic delivery of these immunomodulatory agents (57). More extensive research would also be worthwhile on *S. typhimurium* as a treatment for schwannoma-related neoplasms, including meningiomas and NF1-associated tumors. Translating this therapeutic strategy for clinical use will require understanding differences in host–bacterium interactions between preclinical models and humans, including ex vivo experiments with human tumor tissue. Such knowledge will drive the further engineering of attenuated *S. typhimurium* strains to maximize their clinical efficacy and safety.

Materials and Methods

Bacterial Culture. Wild type (cat# 14028) and attenuated VNP20009 (also denoted YS1646, cat# 202165) *Salmonella* enterica serovar *typhimurium* strains were purchased from American Type Culture Collection (ATCC). Karsten Tedin (Institute for Microbiology and Epizootics, Centre for Infection Medicine, Berlin, Germany) provided attenuated strain ΔppGpp. See *SI Appendix* for more strains and further details.

Data Analysis. All group values are presented as mean ± SEM. To compare outcomes across groups, we computed ANOVA [repeated-measures ANOVA for tumor volumes and signals (58) with Bonferroni post hoc corrections for pairwise comparisons; one-way ANOVA for cytokine expression and flow cytometric data]. We considered $P < 0.05$ as significant. We performed these analyses in GraphPad Prism and Microsoft Excel.

Data Availability. Next-generation sequencing data have been deposited in National Center for Biotechnology Information Sequence Read Archive as accession number PRJNA826093 . All other data are included in the article and/or supporting information.

ACKNOWLEDGMENTS. We thank Drs. Karsten Tedin, Marco Giovannini, David Largaespada, Timothy P. Cripe, Long-Sheng Chang, and G. Yancey Gillespie for kindly sharing biological materials. We thank Drs. Tim Ahern, Dirk Brockstedt, and Giulia Fulci (in alphabetical order) for feedback on the manuscript. We thank Drs. Phanidhar Kukutla and Ahmed Abdelnabi for their technical assistance. Funding for this work came from the Department of Anesthesia, Critical Care and Pain Medicine at Massachusetts General Hospital and charitable donations from Neurofibromatosis Northeast and NF2 BioSolutions to the Rebecca Grasso Fund, and X.W.: R01CA226981-01A1 (X.W.), W81XWH-20-PCRP-IDA (X.W.). During the early phase of the reported work, G.J.B. and S.G.A. received salary support from Grant No. R01-NS081146 from the National Institute of Neurological Disorders and Stroke (NINDS); generation of Fig. 6 data and final manuscript preparation were supported by Grant No. R41NS120338, also from NINDS.

Author affiliations: [a]Department of Anesthesiology, Critical Care, and Pain Medicine, Massachusetts General Hospital, Harvard Medical School, Boston, MA 02144; [b]Department of Microbiology, Harvard Medical School, Boston, MA 02115; and [c]Division of Surgical Oncology, Department of Surgery, Massachusetts General Hospital, Harvard Medical School, Boston, MA 02114

Author contributions: S.G.A., X.W., J.J.M., and G.J.B. designed research; S.G.A., G.O., and M.S. performed research; S.G.A., G.O., J.J.M., and G.J.B. analyzed data; S.G.A. and G.J.B. initially conceptualized the studies; G.O. assisted with manuscript preparation; X.W. and J.J.M. revised manuscript; and S.G.A. and G.J.B. wrote the paper.

Reviewers: S.M., University of Washington; and D.P., University of California Berkeley.

1. C. Lu-Emerson, S. R. Plotkin, The neurofibromatoses. Part 2: NF2 and schwannomatosis. *Rev. Neurol. Dis.* **6**, E81–E86 (2009).
2. D. G. Evans, Neurofibromatosis type 2 (NF2): A clinical and molecular review. *Orphanet J. Rare Dis.* **4**, 16 (2009).
3. H. Inoue *et al.*, Acute brainstem compression by intratumoral hemorrhages in an intracranial hypoglossal schwannoma. *Leg. Med. (Tokyo)* **15**, 249–252 (2013).
4. B. R. Korf, Neurofibromatosis. *Handb. Clin. Neurol.* **111**, 333–340 (2013).
5. M. G. Fehlings *et al.*, Risk factors for recurrence of surgically treated conventional spinal schwannomas: Analysis of 169 patients from a multicenter international database. *Spine* **41**, 390–398 (2016).
6. H. K. Wong *et al.*, Anti-vascular endothelial growth factor therapies as a novel therapeutic approach to treating neurofibromatosis-related tumors. *Cancer Res.* **70**, 3483–3493 (2010).
7. R. A. Lafayette *et al.*, Incidence and relevance of proteinuria in bevacizumab-treated patients: Pooled analysis from randomized controlled trials. *Am. J. Nephrol.* **40**, 75–83 (2014).
8. W. B. Coley, The treatment of malignant tumors by repeated inoculations of erysipelas. With a report of ten original cases. 1893. *Clin. Orthop. Relat. Res.* **262**, 3–11 (1991).
9. M. Wen *et al.*, Targeting orthotopic glioma in mice with genetically engineered *Salmonella typhimurium*. *J. Korean Neurosurg. Soc.* **55**, 131–135 (2014).
10. J. E. Kim *et al.*, *Salmonella typhimurium* suppresses tumor growth via the pro-inflammatory cytokine Interleukin-1β. *Theranostics* **5**, 1328–1342 (2015).
11. J. H. Zheng *et al.*, Two-step enhanced cancer immunotherapy with engineered *Salmonella typhimurium* secreting heterologous flagellin. *Sci. Transl. Med.* **9**, eaak9537 (2017).
12. K. Miyake *et al.*, Tumor-targeting *Salmonella typhimurium* A1-R suppressed an imatinib-resistant gastrointestinal stromal tumor with c-kit exon 11 and 17 mutations. *Heliyon* **4**, e00643 (2018).
13. Y. Guo *et al.*, Targeted cancer immunotherapy with genetically engineered oncolytic *Salmonella typhimurium*. *Cancer Lett.* **469**, 102–110 (2020).
14. T. Kiyuna *et al.*, Tumor-targeting *Salmonella typhimurium* A1-R inhibits osteosarcoma angiogenesis in the *In Vivo* Gelfoam® assay visualized by color-coded imaging. *Anticancer Res.* **38**, 159–164 (2018).
15. M. Yang, J. Xu, Q. Wang, A. Q. Zhang, K. Wang, An obligatory anaerobic *Salmonella typhimurium* strain redirects M2 macrophages to the M1 phenotype. *Oncol. Lett.* **15**, 3918–3922 (2018).
16. M. Dougan, S. K. Dougan, Programmable bacteria as cancer therapy. *Nat. Med.* **25**, 1030–1031 (2019).
17. J. F. Toso *et al.*, Phase I study of the intravenous administration of attenuated *Salmonella typhimurium* to patients with metastatic melanoma. *J. Clin. Oncol.* **20**, 142–152 (2002).
18. J. Nemunaitis *et al.*, Pilot trial of genetically modified, attenuated *Salmonella* expressing the *E. coli* cytosine deaminase gene in refractory cancer patients. *Cancer Gene Ther.* **10**, 737–744 (2003).
19. N. Swietek, M. Waldert, M. Susani, G. Schatzl, T. Klatte, Intravesical bacillus Calmette-Guérin instillation therapy for non-muscle-invasive bladder cancer following solid organ transplantation. *Wien. Klin. Wochenschr.* **125**, 189–195 (2013).
20. R. Tamura *et al.*, The role of vascular endothelial growth factor in the hypoxic and immunosuppressive tumor microenvironment: Perspectives for therapeutic implications. *Med. Oncol.* **37**, 2 (2019).
21. R. Tamura *et al.*, Difference in the hypoxic immunosuppressive microenvironment of patients with neurofibromatosis type 2 schwannomas and sporadic schwannomas. *J. Neurooncol.* **146**, 265–273 (2020).
22. S. Wang *et al.*, Programmed death ligand 1 expression and tumor infiltrating lymphocytes in neurofibromatosis type 1 and 2 associated tumors. *J. Neurooncol.* **138**, 183–190 (2018).
23. C. Cunningham, J. Nemunaitis, A phase I trial of genetically modified *Salmonella typhimurium* expressing cytosine deaminase (TAPET-CD, VNP20029) administered by intratumoral injection in combination with 5-fluorocytosine for patients with advanced or metastatic cancer. Protocol no: CL-017. Version: April 9, 2001. *Hum. Gene Ther.* **12**, 1594–1596 (2001).
24. S. G. Ahmed, A. Abdelanabi, M. Doha, G. J. Brenner, Schwannoma gene therapy by adeno-associated virus delivery of the pore-forming protein Gasdermin-D. *Cancer Gene Ther.* **26**, 259–267 (2019).
25. S. G. Ahmed *et al.*, Gene therapy with apoptosis-associated speck-like protein, a newly described schwannoma tumor suppressor, inhibits schwannoma growth in vivo. *Neuro Oncol.* **21**, 854–866 (2019).
26. K. B. Low *et al.*, Lipid A mutant *Salmonella* with suppressed virulence and TNFα induction retain tumor-targeting in vivo. *Nat. Biotechnol.* **17**, 37–41 (1999).
27. C. Clairmont *et al.*, Biodistribution and genetic stability of the novel antitumor agent VNP20009, a genetically modified strain of *Salmonella typhimurium*. *J. Infect. Dis.* **181**, 1996–2002 (2000).
28. J. Pizarro-Cerdá, K. Tedin, The bacterial signal molecule, ppGpp, regulates *Salmonella virulence* gene expression. *Mol. Microbiol.* **52**, 1827–1844 (2004).
29. M. Jarosz-Biej *et al.*, M1-like macrophages change tumor blood vessels and microenvironment in murine melanoma. *PLoS One* **13**, e0191012 (2018).
30. L. Suarez-Lopez *et al.*, MK2 contributes to tumor progression by promoting M2 macrophage polarization and tumor angiogenesis. *Proc. Natl. Acad. Sci. U.S.A.* **115**, E4236–E4244 (2018).
31. J. K. Messex, C. J. Byrd, G. Y. Liou, Signaling of macrophages that contours the tumor microenvironment for promoting cancer development. *Cells* **9**, 919 (2020).
32. H. Wajant, The role of TNF in cancer. *Results Probl. Cell Differ.* **49**, 1–15 (2009).
33. L. Ni, J. Lu, Interferon gamma in cancer immunotherapy. *Cancer Med.* **7**, 4509–4516 (2018).
34. T. X. Phan *et al.*, Activation of inflammasome by attenuated *Salmonella typhimurium* in bacteria-mediated cancer therapy. *Microbiol. Immunol.* **59**, 664–675 (2015).
35. K. Tanaka *et al.*, Therapeutic potential of HSP90 inhibition for neurofibromatosis type 2. *Clin. Cancer Res.* **19**, 3856–3870 (2013).
36. S. Wang *et al.*, Intratumoral injection of a CpG oligonucleotide reverts resistance to PD-1 blockade by expanding multifunctional $CD8^+$ T cells. *Proc. Natl. Acad. Sci. U.S.A.* **113**, E7240–E7249 (2016).
37. G. T. Motz, G. Coukos, The parallel lives of angiogenesis and immunosuppression: Cancer and other tales. *Nat. Rev. Immunol.* **11**, 702–711 (2011).
38. C. Li, T. Liu, A. V. Bazhin, Y. Yang, The sabotaging role of myeloid cells in anti-angiogenic therapy: Coordination of angiogenesis and immune suppression by hypoxia. *J. Cell. Physiol.* **232**, 2312–2322 (2017).
39. M. de Vries *et al.*, Tumor-associated macrophages are related to volumetric growth of vestibular schwannomas. *Otol. Neurotol.* **34**, 347–352 (2013).
40. V. M. Lu *et al.*, Efficacy and safety of bevacizumab for vestibular schwannoma in neurofibromatosis type 2: A systematic review and meta-analysis of treatment outcomes. *J. Neurooncol.* **144**, 239–248 (2019).
41. K. Majchrzak *et al.*, Markers of angiogenesis (CD31, CD34, rCBV) and their prognostic value in low-grade gliomas. *Neurol. Neurochir. Pol.* **47**, 325–331 (2013).
42. F. Hayashi *et al.*, The innate immune response to bacterial flagellin is mediated by Toll-like receptor 5. *Nature* **410**, 1099–1103 (2001).
43. Y. Y. Mahller *et al.*, Tissue inhibitor of metalloproteinase-3 via oncolytic herpesvirus inhibits tumor growth and vascular progenitors. *Cancer Res.* **68**, 1170–1179 (2008).
44. K. M. Sane *et al.*, A novel geranylgeranyl transferase inhibitor in combination with lovastatin inhibits proliferation and induces autophagy in STS-26T MPNST cells. *J. Pharmacol. Exp. Ther.* **333**, 23–33 (2010).
45. D. Pachow *et al.*, mTORC1 inhibitors suppress meningioma growth in mouse models. *Clin. Cancer Res.* **19**, 1180–1189 (2013).
46. N. E. Annels, G. R. Simpson, H. Pandha, Modifying the non-muscle invasive bladder cancer immune microenvironment for optimal therapeutic response. *Front. Oncol.* **10**, 175 (2020).
47. N. M. Gandhi, A. Morales, D. L. Lamm, Bacillus Calmette-Guérin immunotherapy for genitourinary cancer. *BJU Int.* **112**, 288–297 (2013).
48. S. M. Crowley, L. A. Knodler, B. A. Vallance, *Salmonella* and the inflammasome: Battle for intracellular dominance. *Curr. Top. Microbiol. Immunol.* **397**, 43–67 (2016).
49. A. S. Akhade *et al.*, Type 1 interferon-dependent repression of NLRC4 and iPLA2 licenses down-regulation of *Salmonella* flagellin inside macrophages. *Proc. Natl. Acad. Sci. U.S.A.* **117**, 29811–29822 (2020).
50. A. M. Gram *et al.*, *Salmonella* flagellin activates NAIP/NLRC4 and canonical NLRP3 inflammasomes in human macrophages. *J. Immunol.* **206**, 631–640 (2021).
51. D. Bierschenk *et al.*, The *Salmonella* pathogenicity island-2 subverts human NLRP3 and NLRC4 inflammasome responses. *J. Leukoc. Biol.* **105**, 401–410 (2019).
52. N. Naseer *et al.*, Human NAIP/NLRC4 and NLRP3 inflammasomes detect *Salmonella* type III secretion system activities to restrict intracellular bacterial replication. *PLoS Pathog.* **18**, e1009718 (2022).
53. H. O'Donnell *et al.*, Toll-like receptor and inflammasome signals converge to amplify the innate bactericidal capacity of T helper 1 cells. *Immunity* **40**, 213–224 (2014).
54. A. Mónaco, S. Chilibroste, L. Yim, J. A. Chabalgoity, M. Moreno, Inflammasome activation, NLRP3 engagement and macrophage recruitment to tumor microenvironment are all required for *Salmonella* antitumor effect. *Cancer Immunol. Immunother.* 10.1007/s00262-022-03148-x. (2022).
55. C. R. Gurbatri *et al.*, Engineered probiotics for local tumor delivery of checkpoint blockade nanobodies. *Sci. Transl. Med.* **12**, eaax0876 (2020).
56. T. Zhao *et al.*, Combination of attenuated *Salmonella* carrying PD-1 siRNA with nifuroxazide for colon cancer therapy. *J. Cell. Biochem.* **121**, 1973–1985 (2020).
57. P. Darvin, S. M. Toor, V. Sasidharan Nair, E. Elkord, Immune checkpoint inhibitors: Recent progress and potential biomarkers. *Exp. Mol. Med.* **50**, 1–11 (2018).
58. J. E. Harris, P. M. Sheean, P. M. Gleason, B. Bruemmer, C. Boushey, Publishing nutrition research: A review of multivariate techniques–Part 2: analysis of variance. *J. Acad. Nutr. Diet.* **112**, 90–98 (2012).